Slow Neutron Resonance Spectroscopy. I. U^{238}†

J. L. Rosen, J. S. Desjardins, J. Rainwater, and W. W. Havens, Jr.
Department of Physics, Columbia University, New York, New York
(Received November 20, 1959)

The results of time-of-flight measurements of U^{238} resonances in the region 90–1300 ev are presented and resonance parameters for levels up to 1000 ev are obtained. Neutron widths for the 55 observed levels and radiation widths for 32 of the stronger levels are deduced. The deduced neutron width distribution is found to be in good agreement with the theoretical prediction of Porter and Thomas for a single channel process, while the level spacing distribution agrees with the "repulsion" formula suggested by Wigner. The average value of the radiation widths was found to be $(24.6\pm0.8)\times10^{-3}$ ev, while the average reduced neutron width and level spacing were found to be $(1.76\pm0.26)\times10^{-3}$ ev and 18.5 ± 1.3 ev, respectively. These values are in good agreement with earlier results reported by other workers. A strength function of $(0.95\pm0.15)\times10^{-4}$ is obtained.

It appears on the basis of their size and number, that several of the weaker levels may be due to p-wave neutrons.

I. INTRODUCTION

THIS is the first of what is expected to be a series of papers giving the results of studies using the Columbia University, Nevis synchrocyclotron spectrometer system which has been described in detail elsewhere.[1] The pertinent features of the system are as follows. A high intensity burst of fast neutrons is produced having ~0.12-μsec duration and a 60 cps repetition rate. A flight path of ~35 meters has been employed with a 2000-channel time of flight analyzer using 0.1-μsec detection interval widths for most measurements which gives 5 to 10 mμsec/meter (full width at half maximum) resolution. U^{238} presents a particularly favorable sample material for testing various theories since there is a single compound nucleus spin state involved. Including the seven levels below 100 ev studied by others, Γ_n values have now been assigned for 55 levels below 1000 ev.

Recent years have brought a considerable sophistication in the theoretical and experimental aspects of neutron resonance spectroscopy. Orders-of-magnitude improvements in source intensities, detector efficiencies, energy resolution, and data handling techniques have been made.[1–4] Theoretical developments have kept pace, demanding data of ever increasing quality and quantity. The rigorous formulation of the R-matrix theory of the reaction process was given by Wigner and Eisenbud,[5,6] The pioneering development of the optical model for neutrons by Feshbach, Porter, and Weisskopf[7] was later extended to include spheroidal shapes and "rounded off" nuclear density distributions at the surface.[8] This has led to an R-matrix theory by Lane, Thomas, and Wigner[6,9] and others with the emphasis on the concept of "giant resonances" in the strength function.

In the original optical model theory using a sharp edge nucleus of $R=1.45A^{\frac{1}{3}}\times10^{-13}$ cm; and $V=-42(1+0.03i)$ Mev for $r<R$, peaks were predicted in the $l=0$ strength function $S_0=\langle\Gamma_n^0\rangle_{Av}/\bar{D}$. (Here $\bar{D}$ is the average level spacing for $l=0$ neutrons incident and $\langle\Gamma_n^0\rangle_{Av}$ the corresponding average of the reduced neutron widths for these levels). These peaks were predicted for small neutron energies, at $A\sim1.5$, 13, 55, and 155. The average of S_0 over a wide enough range of A values was expected to be the so called "black nucleus" value of 1.0×10^{-4}, with larger values in the regions of the giant resonances and smaller values between. A similar $l=1$ strength function can be suitably defined after taking account of an extra E^{-1} factor at low energies due to the centrifugal repulsion effect. The $l=1$ giant resonance peaks are expected to occur at A values corresponding to nuclear radii intermediate between those for $l=0$, since the internal radial wave functions are ~90° retarded in phase at the nuclear surface relative to the corresponding $l=0$ functions. This places p-wave giant resonances near $A=100$ and 240 which could be split by spin-orbit coupling. Saplakoglu, Bollinger, and Coté[10] interpret their results for Nb^{93} in the slow neutron region as mainly being due to p-wave levels for which the

† Supported by the U. S. Atomic Energy Commission.

[1] J. Rainwater, W. W. Havens, Jr., J. S. Desjardins, J. L. Rosen, Rev. Sci. Instr. (May 1960).

[2] D. J. Hughes, *Neutron Cross Sections* (Pergamon Press, New York, 1957); D. J. Hughes, in *American Institute of Physics Handbook* (McGraw-Hill Book Company, New York, 1957).

[3] J. Rainwater, in *Handbuch der Physik*, edited by S. Flügge (Springer-Verlag, Berlin, 1957), Vol. 40.

[4] D. J. Hughes and R. B. Schwartz, *Neutron Cross Sections*, Brookhaven National Laboratory Report BNL-325 (Superintendent of Documents, U. S. Government Printing Office, Washington, D. C., 1958), second edition.

[5] L. Eisenbud and E. P. Wigner, Phys. Rev. **72**, 29 (1947).

[6] A. M. Lane and R. G. Thomas, Revs. Modern Phys. **30**, 257 (1958); G. Breit, in *Handbuch der Physik*, edited by S. Flügge (Springer-Verlag, Berlin, 1959), Vol. 40, Part 1, p. 1.

[7] H. Feshbach, C. E. Porter, and V. F. Weisskopf, Phys. Rev. **96**, 448 (1954).

[8] B. Margolis and E. S. Troubetzkoy, Phys. Rev. **106**, 105 (1957); D. M. Chase, L. Wilets, and A. R. Edmonds, Phys. Rev. **110**, 1080 (1958).

[9] A. M. Lane, R. G. Thomas, and E. P. Wigner, Phys. Rev. **99**, 693 (1955).

[10] A. Saplakoglu, L. M. Bollinger, and R. E. Coté, Phys. Rev. **109**, 1258 (1958).

strength function is unusually large. We have found[11] similar levels in Ag for $E<500$ ev which are probably $l=1$ levels. Bollinger et al.[12] observed a very weak level at 10.2 ev in U^{238} which they suggest may be p wave. We have indicated which of the 55 U^{238} levels below 1000 ev are most apt to be p wave.

When the quadrupole distortions[8] are treated in detail, the giant resonance peaks are split into structures covering a considerable range of A values. This is particularly noted for the region near $A=155$. The value 1.0×10^{-4} for the long-range average (over A) of the strength function is simply a reflection of the size of the surface discontinuity transmission value when an incoming wave of propagation constant k reaches a boundary where the propagation constant abruptly changes to a much greater "inside" K. The large strength function in the giant resonance regions would thus be expected to imply strength functions $\ll10^{-4}$ midway in A between giant resonances, as, for example, U^{238} for $l=0$. Introduction of a diffuse nuclear surface and surface quadrupole distortions modifies this expectation. It is found experimentally that $S_0\approx10^{-4}$ for U^{238}. Other theoretical tests which we make are for the distribution of Γ_n^0 values and for the distribution of level spacings.

II. SAMPLE CONSIDERATIONS AND DATA TAKING

For the studies described in this paper, as for most of those made to date using this system, a self-indication detection method,[1] rather than a "flat detector," was used. A foil (or plate) of natural U metal (99.3% U^{238}) 6 in.$\times$30 in. was suspended perpendicular to the beam path below shielded scintillation detectors. The detectors respond to the (n,γ) capture γ rays yielding peaks for those flight times associated with neutron resonances in U^{238}. A considerable background counting rate was present which was mainly due to the relatively strong natural γ radiation from such a large U sample, and partly due to cyclotron associated background which would also be present for a nonradioactive sample material.

In choosing an appropriate sample thickness, several considerations are involved. For too thin a sample the weak levels would be more apt to be missed in detection. Thus thicker samples are favored to detect weak levels. The maximum resonance response occurs when the sample transmission is near zero for an energy interval about resonance of the order of magnitude of the resolution width. For thicker samples there are always two troubles and a third is present for U. The first of these is the fact that the self-absorption of the capture γ rays in the sample itself becomes progressively more serious as the sample thickness increases. This is complicated also by the fact that the mean penetration thickness, and thus the depth of origin of the capture γ rays, becomes a complicated function of energy for which we only partly correct by having the large 8-in. diameter $\times$8-in. thick plastic scintillation detectors positioned symmetrically (front-back) above the "D" sample foil. More serious is the scattering of neutrons of greater than resonance energy in the sample. If the initial energy is within $4E_0/A$ ($\approx E_0/60$ for U^{238}) of the resonance region, a neutron can lose enough energy to have $E\approx E_0$ after scattering with fair likelihood of capture. When a sample having $(1/n)=82$ barns/atom was used, a few of the stronger levels were very distorted on their high-energy sides. For the bulk of the measurements $(1/n)=425$ barns/atom was used and the effect was relatively unimportant. The third effect for U is also true for any naturally radioactive material for which the source intensity increases with increasing mass of sample. In this respect the thinner sample was much more satisfactory than the the thick sample. The strong cyclotron intensity as a slow neutron source was very important for obtaining information on U. For example, had the slow neutron intensity been weaker by a factor of ten, the peak to background counts ratio would have been much poorer, and even counting ten times as long would not have compensated satisfactorily.

In addition to "D only" counts with the "detector sample" in place, counts were taken where an additional transmission sample (as well as the D sample) was in the neutron path ($D+T$ measurements). By comparing the effects over background for ($D+T$) and for D, one obtains a self-indication transmission measurement. The transmission sample had $(1/n)=475$ barns/atom which is nearly the same as for the D sample.

A total of 22 cycles were obtained for the thinner D and T samples. This represented a total of 44 000 000 timed counts each for D and $D+T$, or 22 000 counts/channel average each for D and $D+T$. This took about 36 hours of cyclotron time. These counts are almost entirely due to background. The background subtracted peak rates were, at best, only of the same order of magnitude as the background. In contrast, ratios of 5 or 10 to 1 are common for nonradioactive materials. About 6 hours of cyclotron time was spent on D and $D+T$ using $(1/n)=82$ barns/atom samples. This provided useful supplementary information in developing the over-all analysis structure for the group of levels but these curves are not shown in this paper. The 22 cycles using the thinner samples were split into two separate portions each containing 11 cycles and the two sets of data were analyzed separately to provide an over-all test of the uncertainties in the conclusions.

III. PRELIMINARY DATA PROCESSING

The U^{238} data which was of principle significance for the determination of level parameters was taken using

[11] S. Desjardins, W. W. Havens, Jr., J. Rainwater, and J. Rosen, Bull. Am. Phys. Soc. 4, 34 (1959).
[12] L. M. Bollinger, R. E. Coté, D. A. Dahlberg, and G. E. Thomas, Phys. Rev. **105**, 661 (1957).

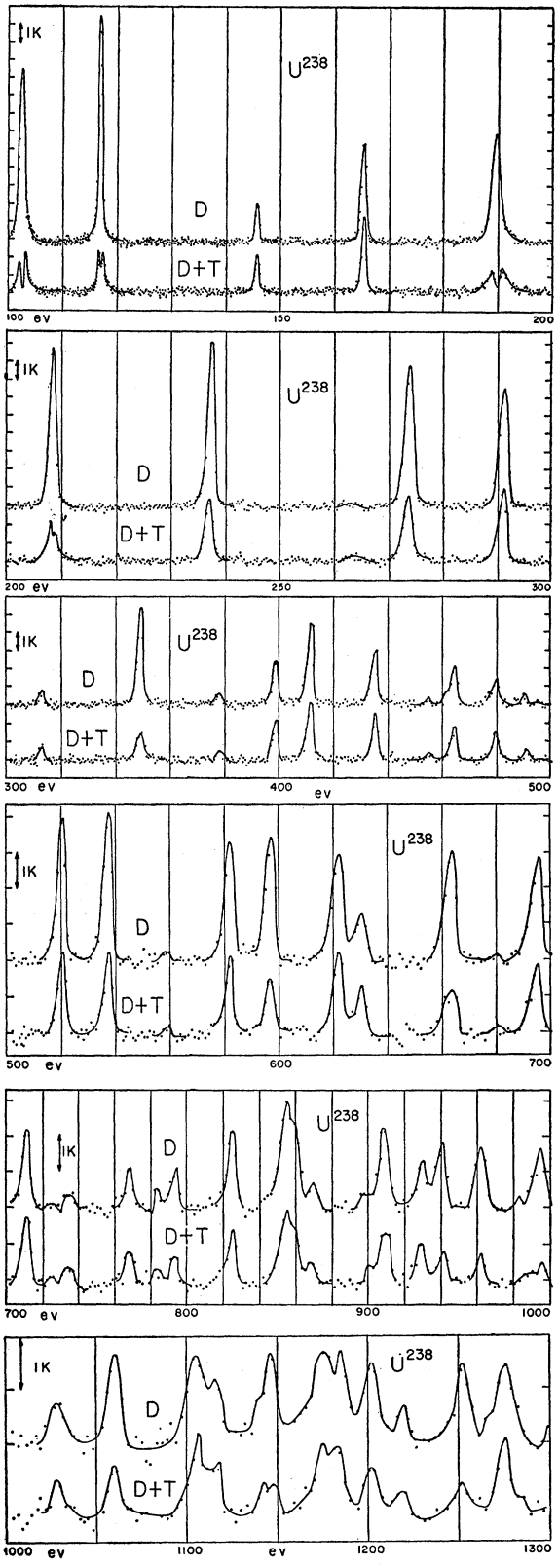

FIG. 1. Background subtracted counts per channel for U^{238}. For the D curve a foil having $n^{-1}=425$ barns/atom at the detector position was viewed by large plastic scintillation detectors to detect (n,γ) capture γ rays. For the $D+T$ curves a sample having $n^{-1}=475$ barns/atom was *also* in a transmission setting. The plots show counts per 0.1-μsec detection interval width for a 35.37 meter neutron path.

the $(1/n)=425$ barns/atom D sample, and $(1/n)=475$ barns/atom T sample. The discussion will sketch the processing of this data only, although we also processed and made use of shorter runs using $n^{-1}=82$ barns/atom samples. The flight path was 35.37 meters, including 1.86 cm to account for the effect of moderation. The group of 2000 detection intervals, each 0.1 μsec wide, was delayed such that the region from 90 ev to 1300 ev was covered. The output data appeared on teletype tape in the form of 2000 five digit octal numbers for each run. These were converted to punched cards and similar D only runs and $D+T$ runs were then combined using an IBM-650 computer to yield four decks of 200 cards each. Two decks had totals for D only with dead time corrections made, multiplied by a proper relative normalization factor to account for differences in the *effective* net running times. The other decks contained similar $D+T$ information.

These data were then printed out and studied. To choose a background function (different for the D and $D+T$ runs), it was assumed that the rate was essentially all due to background at an energy some distance from resonance levels. The background function dropped sharply near $t=0$ (with increasing t) and decreased more gradually at larger timing. It was assumed that a suitable match could be made using a fourth-order polynomial in $x=(999.5-n)$ (where n is the channel number ranging from 0 to 1999), of the form $y=\alpha_0+\alpha_1 x+\alpha_2 x^2+\alpha_3 x^3+\alpha_4 x^4$. The processed data for each interval appeared on one output card containing (a) run identification, (b) interval number, (c) a plotting function linear in the energy, (d) the value of the neutron energy, (e) the total D-only count, (f) the D-only count minus the background function plus 1000 (to avoid negative values), (g) the total $D+T$ count, (h) the background corrected $D+T$ count plus 1000, (i) a running sum of the D only minus background count, and (j) a running sum of the $D+T$ minus background count. Two boxes of 2000 output cards each were obtained for the thinner sample data and a similar box for the thicker sample data.

The D and $D+T$ data were automatically plotted using a Librascope plotter fed by a type 523 IBM Reproducing Punch. Figure 1 shows the D and $D+T$ counts (background subtracted) vs energy for one of the groups of data. Figure 2 indicates the running sums (i) and (j) above, in a limited energy region which includes the level at 597 ev. The discontinuities are due to the fact that the vertical scales are folded at 10 000 where they abruptly change to zero. The relative count "areas" of the peak for D and $D+T$ can be easily read from such a plot and facilitate sub-

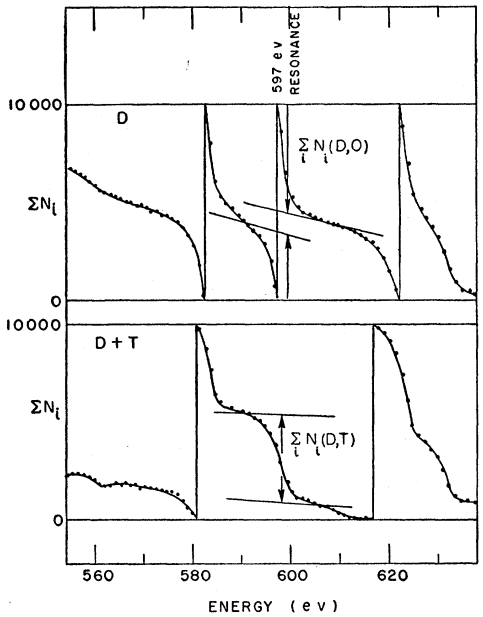

FIG. 2. This shows a selected region of the running sum plots $\Sigma_i N_i(D,0)$ and $\Sigma_i N_i(D,T)$ of the data shown in Fig. 1 in the vicinity of the 597-ev level to illustrate the method of area analysis. The "self-indication transmission," T_{SI}, is the ratio of the lower area to the upper area as discussed in the text. Interval number increases to the left and the curves are folded at 10 000.

sequent analysis. From these plots and inspection of the output card print-out sheets, one can determine the positions of the resonances with an uncertainty given as of-the-order of 0.1 to 0.2% or the spacing between adjacent intervals, whichever is larger. (This is intended to represent a conservative "everything considered" estimate of the energy uncertainty.) These plots also give directly an obvious qualitative indication of a relative level strength from the magnitude of the D peak together with the factor by which it is larger than the $D+T$ peak. Extraction of level parameters such as Γ_n require a more detailed analysis as discussed below. Results for each level were obtained from each of the two sets of thin sample data for comparison.

IV. THEORY AND METHODS OF ANALYSIS

For many elements there are two or more isotopes, each having two different possible compound nucleus spin states for $l=0$ neutrons. This greatly complicates the analysis. One of the reasons for treating U^{238} first is that there is only one spin-zero isotope present with a corresponding great reduction in the problem of analyzing for resonance parameters. The following discussion is therefore specialized to the case of a single spin-zero isotope and $l=0$ neutrons. Before including the effect of Doppler broadening, the cross-section region of a level can be well represented by a single level Breit-Wigner formula with symmetric capture and scattering resonance terms plus terms due to potential scattering and the asymmetric interference term between potential and resonance scattering. The potential scattering has been given by Seth et al.[13] as (10.7 ± 0.3) barns for U^{238}. The interference term is zero at exact resonance and equal but of opposite sign at equal distances below and above E_0 in energy. The over-all effect of the interference term on the measurements is difficult to treat. In first order its effect is zero, and we have ignored it in the analysis. We believe that this introduces no serious errors in the resultant determination of the level parameters. We also usually neglect the effect of events where a first scattering is followed by a resonance capture. This effect was discussed in Sec. II. In the case of a very few levels having extra large Γ_n values small corrections were made. The potential scattering effect is only considered for the $(D+T)$ measurements where it is regarded as reducing the $(D+T)$ peak over background effects. Thus $(D+T)$ counts are divided by the potential scattering transmission value in the choice of a normalization factor, and potential scattering is ignored in the subsequent analysis. This leaves only the Doppler broadened resonance capture and scattering cross-section contributions to be considered.

It has become common for collections of curves showing "measured cross sections" vs energy to be presented.[4] By "measured" is meant that measured transmission curves are directly converted to cross sections by setting $\sigma_{\text{meas}}=(1/n)\ln T_{\text{meas}}^{-1}$. Such cross sections are not corrected for experimental resolution effects, for Doppler broadening, or for sample thickness effects. Since $\ln T_{\text{meas}}^{-1}$ is almost always of the order of magnitude of unity at resonance for detected resonances, the "measured" $\sigma_{\max}$ will almost always be of the order of magnitude of the $(1/n)$ value of the transmission sample. This is why we regard it as most instructive to express sample thickness in terms of $(1/n)$. For the transmission sample $(1/n)=475$ barns/atom, so $\sigma_{\max}$ values are expected to lie within an order of magnitude of this value. The directly obtained values of $\sigma_{\max}$ are given in Table I. Each resonance is defined by a peak involving several intervals, for each of which a σ_{meas} can be obtained (in addition to the single $\sigma_{\max}$ at level center). These additional σ values in the region of each resonance peak are thus also available but are not listed here.

The Doppler broadened resonance total cross section for a single resonance using a simplified perfect gas model[14] is

$$\sigma_t=\sigma_0\psi(\beta,x), \tag{1}$$

where

$$\beta=2\Delta/\Gamma \tag{2}$$

[13] K. K. Seth, D. J. Hughes, R. L. Zimmerman, and R. C. Garth, Phys. Rev. **110**, 692 (1958).

[14] The perfect gas case was treated by H. A. Bethe [Revs. Modern Phys. **9**, 140 (1937)] and the case of a crystalline solid by W. E. Lamb [Phys. Rev. **55**, 190 (1939)]. This is also reviewed in reference 3.

TABLE I. Resonance parameters for U^{238}. Within the framework of the Breit-Wigner single level formula, U^{238} resonances are characterized by three independent parameters. Uncertainties are given for E_0, Γ_n and Γ_γ only. The uncertainty quoted for the resonance energy E_0 is taken to be ~1 channel width. Where Γ_γ was nonmeasurable or known to less than ~30% accuracy, the average value $\Gamma_\gamma=0.0246$ ev was used to obtain values for Γ_n and Γ. The peak resonance cross section, σ_{meas}, is obtained from the ratio of the experimental self-indication curves if this ratio is sufficiently different from one as to be meaningful. In those cases, i.e., the weaker levels, where this was not possible the peak of the D curve and the inferred saturation curve (see text) was used to obtain the peak resonance cross section. Such values are indicated by parenthesis. The parameters for the 7 resonances below 100 ev have been taken from Hughes and Schwartz[a] and represent a compilation of the work of several research groups. Bollinger et al.[b] have observed a resonance at 10.2 ev and suggest that in view of the extremely small Γ_n^0, the level may be p wave. There exists the possibility that some of the other small levels may be p wave, particularly toward the high-energy end of the studied region. For $l=1$ the barrier effect should vary as $(kR^2)=(E/E_B)$ where $E_B\sim300$ kev for U^{238}. Thus Γ_n^0/E_0 is a velocity independent term for p-wave resonances. The levels denoted by an asterisk have $(\Gamma_n^0/E_0)<10^{-7}$ and are thus the most likely p-wave candidates if such are present.

E_0(ev)	$\Delta(10^{-3}$ ev)	σ_{meas}(b)	$\Gamma_n(10^{-3}$ ev)	$\Gamma_\gamma(10^{-3}$ ev)	Γ_n^0	$\Gamma(10^{-3}$ ev)	σ_Δ(b)
6.68±0.06	53.5		1.48±0.05	25±2	0.572	26.5	7800
*10.2±0.1	66.0		0.0014±0.0007		0.0004	25	4.1
21.0±0.3	95.0		9.0±0.3	25±2	1.96	34	8560
36.8±0.6	125.5		33±2	26±4	5.4	59	12900
66.3±1.1	169		23±2	20±3	2.8	43	4120
81.1±1.6	186		2.1±0.2		0.23	27	2960
*90±2	196		0.08±0.01		0.008	25	9.7
102.8±0.1	210	1700	70±5	21±6	6.9	91	6000
117.0±0.1	224	1030	18±3	21±6	1.66	39	1240
145.9±0.1	250	45	0.8±0.2		0.067	25	46
165.7±0.2	267	125	3.5±0.4	14±14	0.27	28	171
190.0±0.2	286	1500	135±15	22±6	9.8	157	4300
209.1±0.2	300	840	55±6	26.5±4	3.8	82	1750
238.0±0.3	320	450	32±4	20.5±4	2.1	53	885
*264.0±0.3	337	(3)	0.23±0.08		0.014	25	6
274.5±0.4	344	350	27±3	22.5±3	1.58	50	605
292.0±0.4	354	235	19±3	19±5	1.11	38	396
312.5±0.4	367	8	1.0±0.2		0.057	26	19
349.0±0.5	387	590	55±10	22±3	2.95	77	860
378±0.6	403	8	1.5±0.3		0.077	26	22
399±0.6	414	63	10±2	40±16	0.5	35	132
412±0.7	421	145	17±3	18±6	0.85	42	213
436±0.7	433	75	14±3	20±8	0.67	39	163
*456±0.8	443	(2.9)	0.7±0.3		0.033	25	8
465±0.8	446	43	7±2	18±14	0.33	32	73
480±0.8	454	17	4.5±0.8	35±25	0.205	29	46
*491±0.9	460	(2.8)	1±0.2		0.045	26	10
520±0.9	473	245	37±6	28.5±4	1.63	66	320
537±1.0	480	285	54±8	24.3±3	2.3	78	442
*558±1.0	490	(1.5)	1±0.3		0.042	26	8
582±1.1	500	210	42±7	23±3	1.74	65	307
597±1.1	506	310	66±10	23±3	2.7	89	382
*606±1.2	510	(2)	0.6±0.3		0.024	25	4.2
622±1.2	517	125	39±6	24±3	1.97	63	273
630±1.2	520	17	9±2		0.36	34	61
663±1.3	534	425	125±20	25.5±3	4.85	151	706
*681±1.4	541	(~2)	1.3±0.3		0.05	26	7.8
696±1.4	547	172	50±10	25.2±3	1.9	75	280
711±1.5	553	90	20±4	33±17	0.75	45	115
*724±1.5	558	(~1)	1.5±0.3		0.055	26	6.5
733±1.6	502	13	4.25±0.9		0.157	29	19
767±1.7	574	17	9±3		0.37	34	46
783±1.7	580	(2.6)	3±0.7		0.107	28	15
793±1.7	585	15	11±3	15±13	0.39	36	53
826±1.9	597	175	60±10	32±5	0.21	92	256
856±2.0	608	200	130±50		4.55	155	505
860±2.0	609	150	60±30		2.05	85	243
*869±2.0	614	10	2.2±0.5		0.075	27	9.1
*898±2.1	622	(~1)	1.3±0.4		0.043	26	5.2
911±2.1	626	180	90±20	34.7±7	3.0	125	324
930±2.2	634	35	37±8		1.21	62	137
942±2.3	637	300	195±40	25±3	6.35	220	622
962±2.3	645	300	190±40	23.5±3	6.15	214	694
*985±2.4	652	(1)	1.0±0.6		0.03	26	3.5
997±2.5	655	460	400±100	30±6	12.7	430	990
E_0(ev)	$\Delta(10^{-3}$ ev)	σ_{meas}(b)	$\Gamma_n(10^{-3}$ ev)	$\Gamma_\gamma(10^{-3}$ ev)	Γ_n^0	$\Gamma(10^{-3}$ ev)	σ_Δ(b)

[a] See reference 4. [b] See reference 12.

is proportional to the ratio of Doppler to natural level width. $\Delta=(4mkTE/M)^{\frac{1}{2}}$ is the Doppler width where m and M are the neutron and nuclear masses, k is Boltzmann's constant, and T is the sample temperature. $\Gamma=\Gamma_\gamma+\Gamma_n$ is the natural level full width at half maximum and Γ_γ and Γ_n are the capture and scattering

partial widths.

$$x=2(E-E_0)/\Gamma \tag{3}$$

and

$$\sigma_0=2.60\times10^6(\text{barns/atom})E_0^{-1}(\Gamma_n/\Gamma) \tag{4}$$

is the peak cross section in the absence of Doppler broadening (where E_0 is in ev).

$$\psi(\beta,x)=1/(\pi)^{\frac{1}{2}}\beta\int_{-\infty}^{\infty}(1+y^2)^{-1}dy\times\exp[-(x-y)^2\beta^{-2}], \tag{5}$$

This function has been most extensively tabulated by Rose et al.[15] $\sigma_\Delta=\sigma_0\psi(\beta,0)$ is the peak cross section in the presence of Doppler broadening and is the quantity to compare with the measured peak cross section to indicate the effect of finite resolution. The relationship between σ_Δ and σ_0 is plotted vs Δ/Γ in Fig. 2 of reference 3. For $0.50\leq\Delta/\Gamma\leq10$ the following relation holds to within $\sim2\%$ or better,

$$\sigma_0\Gamma=(1.11+0.75\Gamma/\Delta)\sigma_\Delta\Delta. \tag{6}$$

Values of σ_Δ and Δ are given in Table I for the observed resonances in U^{238}.

The analysis applied to the self-indication data is based on a suitable adaptation of the area method which was originally developed for the analysis of flat detector transmission data. Before taking resolution effects into account and ignoring potential effects, the sample transmission is simply $T(E)=\exp[-n\sigma_t(E)]$ using Eq. (1) for σ. The area of a transmission dip is

$$A\equiv\int[1-T(E)]dE \tag{7}$$

over the resonance dip. Curves of (A/Δ) vs $n\sigma_0(\Gamma/\Delta)$ have been prepared in a particularly useful form by the Brookhaven slow-neutron cross-section group[16] and have proved to be very useful for our analysis. For thin samples the well-known relation

$$A\approx\pi n\sigma_0\Gamma/2 \text{ applies for } n\sigma_\Delta\ll1. \tag{8}$$

For thick samples the appropriate expression is

$$A\approx[\pi n\sigma_0\Gamma^2]^{\frac{1}{2}} \text{ for } n\sigma_\Delta\gg1. \tag{9}$$

Since the measurements described use "self-indication detection," is is not *a priori* obvious that the theory evolved for "flat detector" measurements can be applied. Since somewhat subtle reasoning is involved, and many bits of information concerning a level must be combined to permit such an analysis, it is helpful in explaining our procedures to approach the general case via prior consideration of simpler, idealized limiting cases.

[15] M. E. Rose, M. Miranker, P. Leak, L. Rosenthal, and J. K. Hendrickson, Westinghouse Electric Corporation, Atomic Power Division, Pittsburgh, WAPD-SR-506 (unpublished).

[16] V. E. Pilcher, J. A. Harvey, and D. J. Hughes, Phys. Rev. **103**, 1342 (1956). The curves are also given in reference 3.

Case A

Suppose the resonance has $\Gamma_n\ll\Gamma_\gamma$ so it is essentially pure capture and at the same time $n\sigma_\Delta\gg1$ so the D-only curve reaches the "*absolute saturation intensity*" $S_a(E)$ associated with the capture of all incident neutrons. Then, assuming in the following discussions that the background rate has been properly subtracted, the count will be $S_a(E_0)[1-T(E)]$ suitably averaged over the experimental resolution function. The background line corresponds to $T=1$ while the $S_a(E_0)$ peak level corresponds to $T=0$. Clearly the D-only curve corresponds to an inverted transmission curve where the $T=0$ and $T=1$ levels are known, so the area method can be applied. The two assumptions are (a) that only capture interactions are present to an important extent, and (b) that the D-only peak is saturated corresponding to $T\approx0$ at resonance. Since the D and T samples are of almost the same thickness, and $D+T$ curve for such a resonance should, because of the action of the T sample, have no counts over background at E_0.

Inspection of Fig. 1 shows that only the levels at 102.8 ev and 190.9 ev satisfy this last criterion and are examples of the effect to be expected. Inspection of Table I also shows that we assign values of $\Gamma_n>\Gamma_\gamma$ to these levels, so this ideal case is not represented by any of the U^{238} levels. The condition of large $\sigma_0\Gamma$ together with very small Γ_n is, in fact, contradicted by Eq. (4).

Case B

For Case B take the situation of the levels at 102.8 ev and 190.0 ev where $T\approx0$ at resonance but where Γ_n is not $\ll\Gamma_\gamma$. Assume, however, that any neutron undergoing resonance scattering will not be captured in a subsequent interaction. More specifically, assume that second or higher order interactions in the sample can be ignored. Then the *relatively* saturated D-only counting rate at peak is $S_r(E_0)=(\Gamma_\gamma/\Gamma)S_a(E_0)$ and the $T=0$ and $T=1$ levels are established to permit area analysis as in Case A.

Note that exactly the same analysis as above could be made if there was a constant probability $p=0$ to 1 of subsequent capture after a resonance scattering. If p were constant over the resonance, (Γ_γ/Γ) would just be replaced by $(\Gamma_\gamma+p\Gamma_n)/\Gamma$ and the $T=0$ and $T=1$ levels would still be known. In an actual situation, p varies over a resonance since, in an $l=0$ scattering, there is equal probability per unit energy for any energy loss between zero and $4E_0/A\approx E_0/60$ for U^{238}. For $E_0>100$ ev this energy tends to be large compared to the level width and is one reason why the method is best for levels $\gtrsim100$ ev in energy. Even though p varies over a level, the peak will still be essentially at E_0. The larger p above resonance will tend to increase the area while the smaller p below exact resonance will tend to give a compensating decrease, resulting in a nearly correct area determination.

One useful and interesting consequence of the above considerations is that, other things being equal, the $T=0$ saturation rate is proportional to (Γ_γ/Γ) if p is small. It may be noted that the saturated D-only peak at 102.8 ev is significantly smaller than the following less saturated peak at 117.0 ev which has a larger (Γ_γ/Γ). Similarly the saturated peak at 190.0 ev is smaller than the next two unsaturated peaks at 209.1 ev and 238.0 ev. The 165.2 ev peak has essentially the same height as the 190.0 ev level despite the fact that T is close to unity at E_0 as seen from the near equivalence of the D and $D+T$ curves. We show later how this effect is made to contribute to the over-all level analysis.

Case C

Inspection of Fig. 1 shows that most of the levels are not saturated, since the $D+T$ curves do not dip to zero at the center of the resonance. If p is regarded as constant over the level, use can be made of a different type of area analysis, which gives a self-indication transmission. This analysis also applies to the case of saturated levels. The integrated counts $\sum N_i(D,0)$ and $\sum N_i(D,T)$ over a resonance are compared. Here $N_i(D,0)$ represents the number of detector counts over the background in the i detection interval for no transmission sample and $N_i(D,T)$ is the similar quantity for the T sample in place. Let A_D represent the area under the transmission curve of the D sample. Let A_T represent the similar area for the T sample and A_{D+T} for the two samples together. Now $\sum N_i(D,0)$ is proportional to A_D. $A_D \equiv \int(1-T_D)dE$ where T_D = transmission of D sample. $\sum N_i(D,0)=CA_D$ where C is the constant of proportionality. $\sum N_i(D,T) = C\int T_T(1-T_D)dE = C[A_{D+T}-A_T]$, thus the self-indication transmission T_{SI} defined as

$$\frac{\sum N_i(D,T)}{\sum N_i(D,0)} \equiv T_{SI} = \frac{(A_{D+T}-A_T)}{A_D} \qquad (10)$$

is represented theoretically in terms of the ratio of $(A_{D+T}-A_T)$ to A_D. Curves of T_{SI} have been prepared from the basic curves of A/Δ vs $n\sigma_0\Gamma/\Delta$ for various ratios of n_D to n_T including the ratio used for U^{238} where n_D is nearly equal to n_T.

Figure 3 shows a plot of T_{SI} vs $n\sigma_0\Gamma/\Delta$ for the equal thickness case. The curves approach unity as $n\sigma_0\Gamma \to 0$ and approach the fixed value $[\sqrt{2}-1]$ for very large $n\sigma_0\Gamma/\Delta$. These effects are related to the fact that A is linear in n for small n and varies as $\sqrt{n}$ for very large n.

The decrease in T_{SI} below unity is an indication of the deviation from linearity of the area as a function of the thickness. If the average logarithmic slope between n and $2n$ is s, then $T_{SI}=[2^s-1]$. For $\Delta/\Gamma \ll 1$ the value of s changes monotonically from $s=1$ to $s=\frac{1}{2}$, but for $\Delta/\Gamma \gg 1$ the effective value of s becomes much smaller than $\frac{1}{2}$ for intermediate values of $n\sigma_0\Gamma/\Delta$ ~ 10 to 30. Since $\Delta/\Gamma \sim 10$ is common for the U^{238} levels above 100 ev, this represents a region of Δ/Γ values actually encountered.

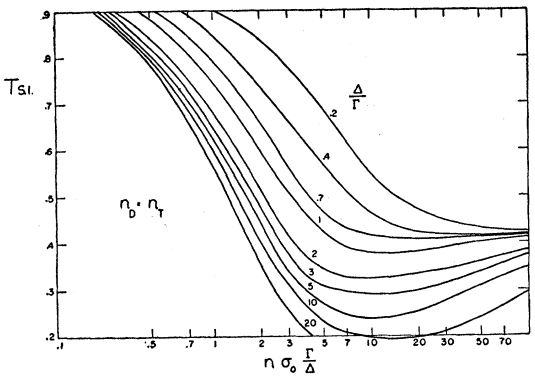

FIG. 3. Calculated curves showing the expected dependence of T_{SI} on $n\sigma_0\Gamma/\Delta$ for various choices of Δ/Γ for the special case of equal D and T sample thicknesses. For large $n\sigma_0\Gamma/\Delta$ the curves converge to $[\sqrt{2}-1]$.

For each Δ/Γ greater than that which gives the measured $T_{SI}<0.4$ as the minimum of its curve, there are two values of $n\sigma_0\Gamma/\Delta$ which satisfy the measured T_{SI}. In most cases, however, other information tends to either (a) restrict the $n\sigma_0\Gamma/\Delta$ values to a small region on the left half of the figure where curves of different reasonable Δ/Γ are close together, or (b) suggest that $n\sigma_0\Gamma/\Delta$ is near the region minima and thus restrict Δ/Γ as being essentially that value which has its curve minimum equal to the measured T_{SI}. In any event, use of T_{SI} is very helpful for the analysis.

The fact that the logarithmic slope s becomes much smaller than its asymptotic values for intermediate $n\sigma_0\Gamma/\Delta$ is understood as follows. For $\Delta=0$ the Breit Wigner formula has a slow drop off in the edges. In the center $n\sigma \gg 1$ merely means $(1-T)\approx 1$ whether $n\sigma \sim 3$ or ~ 100. The Gaussian shape is characterized by a much faster drop off at the edges. Thus for a range of $n\sigma_0\Gamma/\Delta$ values, and large Δ/Γ, the supersaturated peak central region is spread out to a width of a few Δ, over which $(1-T)\approx 0$, but with a sharp recovery to $T\approx 1$ beyond. A factor of two increase in n does not produce much change in the position of the edge transition region, so the area can reach an almost stationary value until $n\sigma_0\Gamma^2$ becomes large enough that the Breit-Wigner wings again dominate in determining the area.

V. ANALYSIS OF RESONANCE PARAMETERS FOR U^{238}

It has turned out that development of the system of level parameters for a sample tends to be a cooperative group process. By this it is meant that information from many levels is combined to provide better information on the function $S_a(E)$, the absolute saturation intensity, which is then used to obtain better evaluation of the parameters of individual resonances than would be obtained using information available for each

resonance alone. The method by which this is accomplished is discussed below.

It has been noted above how the D-only curves are essentially inverted transmission curves where $T=0$ corresponds to some relative saturation rate $S_r(E_0)$ which differs for each level. From Eq. (4) it is seen that there is direct relation between the level strength and Γ_n such that weak levels have small Γ_n and $\Gamma\approx\Gamma_\gamma$, while strong levels have large Γ_n. For very weak levels S_r should be essentially equal to S_a. In the systematic analysis of the levels, the thin sample data was used first as follows:

(1) For all levels where T_{SI} was $\sim$0.5 to 0.9, various reasonable choices of Γ_γ in the region of the mean $\Gamma_\gamma\approx25$ mb reported from low-energy resonances were tried. Each assumed Γ_γ gave an $n\sigma_0\Gamma/\Delta$, or Γ_n, reasonably insensitive to Γ_γ in this range.

(2) The value Γ_n obtained implies a definite A_D for the D-only curve. This in turn requires a definite $S_r(E_0)$ for the level which is then determined for each choice of Γ_γ. Each choice of Γ_γ similarly implies a value for S_a.

(3) For saturated, or nearly saturated, levels for which S_r values can be immediately established, the value of A_D is determined, and thus $\sigma_0\Gamma$, or Γ_n, is obtained for each trial value of Γ_γ. Each trial Γ_γ thus also implies a value of S_a.

(4) Many levels having $T_{SI}\approx1$ for the *thin* samples had "favorable" T_{SI} values for the *thick* sample measurements permitting Γ_n vs Γ_γ to be determined. Thus, for each choice of Γ_γ, an A_D value is predicted for the *thin* sample D-only curve which requires a definite S_r for the *thin* sample curve. Similarly, for each assumed choice of Γ_γ, an $S_a\approx S_r$ value is implied for the *thin* sample, where the value is relatively insensitive to Γ_γ for Γ_γ within a factor of two of 0.025 ev.

(5) After examining the resulting set of $S_a(E($ values it was noted that they are consistent with all being given by a common relation $S_a=1870E^{0.6}$ counts/interval, where E is in ev.

For those levels for which S_a was determined with reasonable accuracy, the S_a values were never far from this curve. S_a depends on the net probability of detecting γ rays emitted in a capture and should in principle depend on the particular γ-ray cascade by which the 4.6-Mev binding is emitted. Even though this sequence probably differs significantly for different levels,[17] there is evidence from other elements as well as U^{238} that our detection probability for the capture event is roughly proportional to the emitted total γ-ray energy (neutron binding) and is relatively insensitive to the variations from level to level. We thus adopted the common curve $S_a=1870E^{0.6}$ to apply for all levels. The $E^{0.6}$ factor gives the spectrum shape for equal Δt intervals.

[17] T. E. Springer and J. E. Draper, Bull. Am. Phys. Soc. 4, 35 (1959).

Once S_a is known, the value S_a, together with the value S_r and Γ_n for the level provide a good determination of Γ_γ for the level. *All of the 28 radiation widths listed in Table I for levels above 100 ev were obtained by this method.* The method also permits determination of A_D, and thus of Γ_n for very weak levels for which $T_{SI}\approx1$.

Table I gives the values for the level parameters for the levels (starting with that at 102.8 ev) determined by these measurements, together with values previously reported for levels at lower energies for completeness. The stated uncertainties represent standard deviations implied by statistical uncertainties. The indicated value of Γ_γ was only used in determining Γ if its uncertainty was less than 30%. Otherwise the average value $\bar{\Gamma}_\gamma=24.6$ millivolts was used.

Example of Analysis Methods Applied to the 597 ev Level

The analysis for the 597-ev level was made using only the thin sample data. The areas $\sum N_i(D,0)$ and $\sum N_i(D,T)$ were obtained from the running sum plots of Fig. 2. The sums increase monotonically going from right to left, but are folded each time they cross 10 000. Thus the ordinate at $\sim$590 ev should be $\sim$9000 above the ordinate at $\sim$600 ev for the upper curve. The level is where the curves have maximum slope (excluding folding discontinuities). If the chosen smooth background function were believed to give a completely correct background correction near the 597-ev level, the change in ordinate between the midpoint P_1 between the 597- and 622-ev level and the

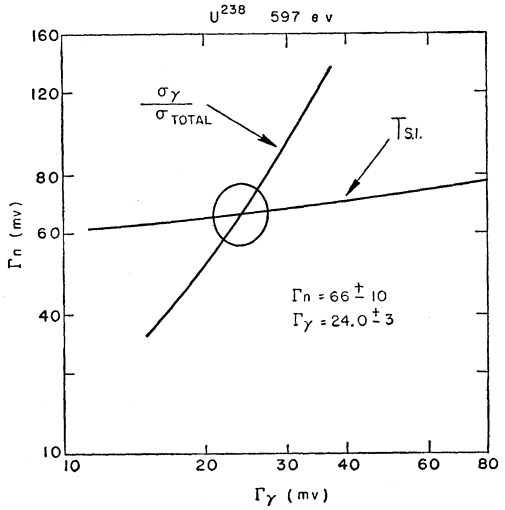

FIG. 4. This shows an example of the method of determining level parameters using the 597-ev level. The measured T_{SI} (see Fig. 2) implies a definite Γ_n (curve labelled T_{SI}), A_D, and S_r for each choice of Γ_γ. A different Γ_n is implied from $S_r=(\Gamma_\gamma/\Gamma)S_a$, where $S_a=1870E^{0.6}$. This gives the second curve vs Γ_γ. The point of intersection determines Γ_n and Γ_γ within an uncertainty given by the error ellipse.

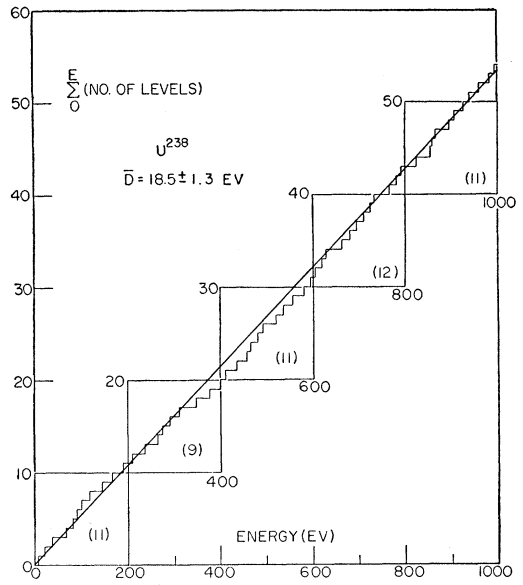

FIG. 5. The sum $E=0$ to E of the number of observed resonances in U^{238} to energy E. The slope of the curve yields the average level spacing $\bar{D}$. The number of resonances contained in the indicated energy sub-intervals are shown in brackets.

midpoint P_2 between 582- and 597-ev levels would represent $\sum N_i(D,0)$. Instead, straight lines are drawn through P_1 and P_2 which have about the same slope as the curve near 570 ev, where its slope is a relative minimum. The spacing between the lines, including 10 000 units of folding, then gives a "corrected" $\sum N_i(D,0)$. A similar method is used for the lower curve.[18] Other wing correction methods are also used sometimes depending on the behavior of the curves in the region of the given level.

Figure 4 shows the plot of Γ_n vs Γ_γ obtained from T_{SI}. For each trial Γ_γ on this curve, a value of A_D, and thus S_r is implied. Using this S_r and the standard S_a implies Γ_γ/Γ to give the second intercepting curve. The crossing determines the best choice of parameters and the ellipse indicates the probable error limits. Good Γ_γ values are only obtained when the curves cross at a steep angle. Inspection of Table I confirms the remark that this only occurs where Γ_γ/Γ is significantly different from unity. This requires a reasonably large Γ_n.

VI. RESULTS AND DISCUSSION

The results of the data analysis covering the region 100–1000 ev are listed in Table I. The aggregate of measured widths and energies represent a considerable increase over previous work which extended to ~250 ev. This is particularly true of the set of radiation widths where the number of measured Γ_γ has been extended from 4 to 32. $\Gamma_n^0 \equiv \Gamma_n[E_0(\text{ev})]^{-\frac{1}{2}}$ is more useful than Γ_n for the purpose of comparing different resonances, since it is an intrinsically velocity-independent quantity. The physical importance of Γ_n^0 lies in the fact that it is proportional to the square of the matrix element which describes the surface overlap between the eigenfunction for the state of the compound nucleus and the wave function for the neutron channel. In terms of the Wigner-Eisenbud reaction theory, this matrix element is a "surface" integral in the nuclear $3A$-dimensional configuration space with the "channel radius" defining the surface.

Because of the complexity of the nuclear many-body problem, it is by considering aggregates of resonances that information of theoretical interest can best be obtained. A discussion of neutron resonance systematics readily splits into two topics: the relation of certain "gross-structure" quantities to nuclear models, and the nature of the fluctuations, correlations, and distributions that may relate to the resonance parameters.

Figure 5 displays a histogram of the integral distribution of the number of resonances vs neutron energy. It is clear that the slope of the inferred curve provides the average level density, or the inverse quantity, the average level spacing $\bar{D}$. Since the energy change over this region is very much smaller than the 4.6-Mev excitation energy of the compound nucleus, one naturally expects the level density to be essentially constant except for fluctuation effects. Thus, this type of plot also serves as a check on the instrumental ability to detect and resolve levels. If extended above 1 kev, the slope of the histogram would begin to decrease, indicating a failure to observe levels.

The integral distribution of the reduced widths vs neutron energy is plotted in Fig. 6. The slope of this curve provides the "strength function" $\langle\Gamma_n^0\rangle_{Av}/\bar{D}$. This quantity is related to the penetrability of the nuclear surface. Specifically, the average $l=0$ cross section for compound nucleus formation is

$$\sigma_c = 2\pi^2 \lambda\!\!\!^{-2} E^{-\frac{1}{2}} \langle\Gamma_n^0\rangle_{Av}/\bar{D}.$$

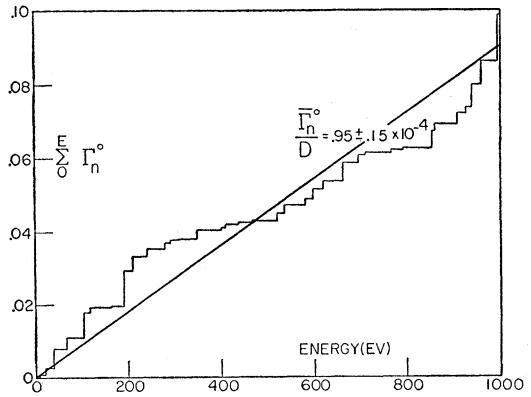

FIG. 6. The sum $E=0$ to E of the Γ_n^0 values for observed levels. The slope of this curve determines the strength function $\langle\Gamma_n^0\rangle_{Av}/\bar{D}$.

[18] The use of this type of plot was first suggested to us by Dr. E. Melkonian.

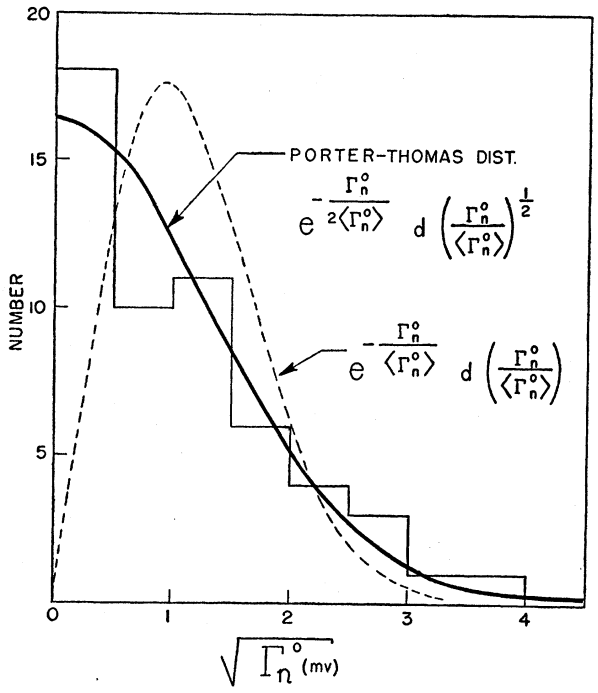

FIG. 7. The distribution of reduced witdh amplitudes $(\Gamma_n^0)^{\frac{1}{2}}$ per 0.5 $(10^{-3}$ ev$)^{\frac{1}{2}}$ interval for 54 resonances in U^{238} from 0 to 1000 ev. The smooth solid curve represents the Porter-Thomas distribution ($\nu=1$) while the dashed curve corresponds to a random distribution of reduced widths ($\nu=2$).

The present measurement $\langle\Gamma_n^0\rangle_{Av}/\bar{D}=(0.95\pm0.15)\times10^{-4}$ agrees well with the value of $(1.15\pm0.15)\times10^{-4}$ obtained by Hughes, Zimmerman, and Chrien.[19] Their value is a weighted average of the result obtained from the low-energy resonances and a measurement of σ_c in the region of a few kev. The data has been examined for the occurrence of a short range correlation, i.e., a correlation between Γ_n^0 and the local level spacing. No evidence of such an effect has been found.

The precision measure of $\bar{\Gamma}_\gamma$ is $(24.6\pm0.8)\times10^{-3}$ ev. It is again emphasized that the Γ_γ inferred entirely or in part from the capture cross section, reflect the intrinsic fluctuation of the detector efficiency in addition to the measurement uncertainty. Almost all of the 32 measured values are within their standard deviations from the average value which, for 22 levels, is less than 30%. This is consistent with the fact that the radiation width is the sum of a large number of partial widths describing the individual transitions to the lower lying states. The effective number of independently contributing partial widths is also large, and statistical arguments such as those advanced by Porter and Thomas[20] indicate the variation of the Γ_γ should be small. Effects due to intrinsic variations were neglected in giving the above stated uncertainty.

[19] D. J. Hughes, R. L. Zimmerman, and R. E. Chrien, Phys. Rev. Letters 1, 461 (1958).
[20] C. E. Porter and R. G. Thomas, Phys. Rev. **104**, 483 (1956).

The deduced gross structure parameters of U^{238} are given in Table II using our data together with that of others.

Consider now the experimental nuclear width and spacing distributions. The distribution of the 54 reduced width amplitudes, $(\Gamma_n^0)^{\frac{1}{2}}$ is plotted in Fig. 7. The Porter-Thomas distribution for one channel, $\nu=1$, is seen to provide an excellent fit while the exponential distribution, corresponding to $\nu=2$, is unsatisfactory. For an arbitrary number of neutron channels ν, the expected shape is (unnormalized) $P(\Gamma_n^0)d\Gamma_n^0=(\Gamma_n^0)^{(\nu-2)/2}\exp(-\nu\Gamma_n^0/2\langle\Gamma_n^0\rangle_{Av})d\Gamma_n^0$. A maximum likelihood analysis gives $\nu=1.06\pm0.16$ for the U^{238} data where no correction was made for the possible failure to observe extremely weak levels. Similarly, Fig. 8 indicates how the Wigner distribution best describes the experimental level spacing distribution, while the random distribution function does not. This result is in agreement with the data inferred from other elements.[21] Note that the Wigner distribution predicts not only considerably less small spacings but fewer very large spacings as well. The comparative excellence of the fit for both spacings and reducted widths reinforces the belief that, at most, very few small levels or small spacings are unobserved.

The opposite viewpoint, that some of the very small reduced widths may belong to a different distribution; namely, that of the p-wave resonances is worth considering.

Bollinger et al.[12] have suggested that the level at 10.2 ev, in view of its extremely small size, may be p wave. Following Saplakoglu et al.,[10] a p-wave strength function S_1 is defined by requiring that it play the analogous role as $\langle\Gamma_n^0\rangle_{Av}/\bar{D}$ does for s-wave neutrons in determining the average cross section for compound nucleus formation.

$$\langle\sigma_c^1\rangle_{Av}=2\pi^2\lambda^2E^{\frac{1}{2}}\frac{x^2}{1+x^2}(2l+1)S_1. \tag{13}$$

Here $x=kR$, where R is the nuclear radius. Note that R is not equal to the potential scattering radius R', but is related to it by a suitable nuclear model.[13,22] Here no distinction has been made between the $l=1$ states $J=\frac{1}{2}$ and $\frac{3}{2}$ for simplicity. It can be shown that S_1 is related to the individual resonances by

$$S_1=(2l+1)^{-1}\langle g\Gamma_n^1\rangle_{Av}/\bar{D}_1 \tag{14}$$

TABLE II. Gross structure parameters of U^{238}.

1.	$\langle\Gamma_n^0\rangle_{Av}/\bar{D}=(\ 0.95\pm0.15)\times10^{-4}$
2.	$\langle\Gamma_n^0\rangle_{Av}=(\ 1.76\pm0.26)\times10^{-3}$ ev
3.	$\bar{\Gamma}_\gamma=(24.6\ \pm0.8\ )\times10^{-3}$ ev
4.	$\sigma_p=(10.7\ \pm0.3\ )$ b
5.	$\bar{D}=(18.5\ \pm1.3\ )$ ev

[21] J. A. Harvey and D. J. Hughes, Phys. Rev. **109**, 471 (1958).
[22] D. M. Chase, L. Wilets, and A. R. Edmonds, reference 8.

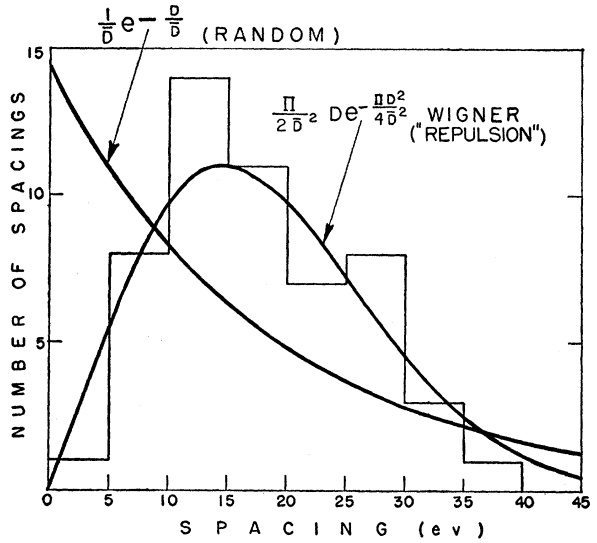

FIG. 8. The distribution of level spacings per 5 ev interval for the first 54 level spacings in U^{238} from 0 to 1000 ev. The smooth curves represent the "repulsion" formula proposed by Wigner and an exponential function corresponding to a random distribution of spacings.

where $\Gamma_n^1 \equiv \Gamma_n E_0^{-\frac{1}{2}}(x_0^2+1)x_0^{-2}$, with E and x evaluated at the resonance energy. The statistical weight factor $g=\frac{1}{2}(2J+1)(2I+1)^{-1}$ with I the spin of the target nucleus and J the spin of the compound nucleus. $g=1$ or 2 for $J=\frac{1}{2}$ or $\frac{3}{2}$. $\bar{D}_1$ is the average $l=1$ level spacing.

The potential barrier factor $(kR)^2=E(\text{ev})/300$ kev for U^{238} using the value $R=(8.4\pm0.1)$ fermis of reference 13. It is seen that the ratios $\Gamma_n^0/\langle\Gamma_n^0\rangle_{Av}$ for a few of the small levels of the present data are of the order-of-magnitude of $(kR)^2$. The comparatively good fits of the Porter-Thomas and Wigner distributions would not be impaired if ~ 4 of the smallest levels were attributed to p-wave neutrons.

However, if ~ 14 of the weaker levels (in Γ_n^0/E_0) were attributed to p-wave levels, the exponential distribution in s-wave Γ_n^0 values could give a better fit than the Porter-Thomas function for $\nu=1$. The value of $\langle\Gamma_n^0\rangle_{Av}$ for s-wave levels increases in proportion to the fraction of weak levels called p-wave levels.

One should consider the expected behavior of S_1. The optical model[7] predicts a maximum for S_1 in just this region of atomic number A which makes the p-wave interpretation of the weaker levels all the more plausible. This may however, be naive in that it does not consider the possible splitting and reduction effects of the spin-orbit coupling and nuclear distortion.

VII. ACKNOWLEDGMENTS

The authors wish to acknowledge the important contributions of J. Hahn and his staff for the engineering and design work on the 2000 channel analysis system. The aid furnished by the velocity selector technicians, A. Blake, D. Passman, and G. Peterson is gratefully acknowledged. The authors are also indebted to Dr. E. Melkonian for discussions concerning analysis methods.

The Nevis synchrocyclotron is a facility of Columbia University and the Joint Program of the Office of Naval Research and the Atomic Energy Commission.